AlGaInAs intracavity selective absorber for an efficient high-power Nd:YAG laser operation at 1.44 μm

Y. P. Huang, Y. T. Chang, K. W. Su, Y. F. Chen,* and K. F. Huang

Department of Electrophysics, National Chiao Tung University, Hsinchu, Taiwan
**Corresponding author: yfchen@cc.nctu.edu.tw*

Received April 14, 2008; accepted May 16, 2008;
posted May 27, 2008 (Doc. ID 94981); published June 23, 2008

We develop an AlGaInAs material as a promising intracavity selective absorber for an efficient high-power Nd:YAG laser at 1.44 μm. With the ISA to suppress operation at 1.06 μm, the output coupler at 1.44 μm can be straightforwardly designed and optimized. At a pump power of 16 W an output power of 2.5 W at 1.44 μm, with a slope efficiency of 23%, was achieved. © 2008 Optical Society of America

OCIS codes: 140.0140, 140.3480, 140.3380, 140.3530.

The fluorescence spectra of Nd-doped laser crystals have revealed many transitions in the $^4F_{3/2}$ to $^4I_{9/2}$, $^4I_{11/2}$, and $^4I_{13/2}$ manifolds [1]. Based on these multiple transitions most Nd-doped laser crystals can be operated in the laser wavelengths between 0.91 and 1.38 μm. In Nd:YAG crystals the long-wavelength end of the $^4F_{3/2} \rightarrow {}^4I_{13/2}$ transition is remarkably up to 1.44 μm at which the absorption coefficient of water is comparable with that at 2.1 μm [2]. As a consequence, the Nd:YAG laser at 1.44 μm is of particular interest not only in the field of surgery but also for many technical applications such as lidar and communications [3–5].

The well-known attempts at line selection in Nd-doped lasers rely on appropriately coated cavity mirrors with a sufficiently large loss difference to suppress the competing transition channels [6]. Since the stimulated emission cross section of the 1.44 μm transition is approximately 20 times smaller than that of the 1.06 μm line, the operation of a Nd:YAG laser at 1.44 μm requires a rather tough coating. Even though the coated cavity mirrors with a sufficient reflection contrast can lead to the 1.44 μm emission at low and middle pump powers, the power scaling tends to be hindered by the lasing of the 1.06 μm transition at high pump powers. A method for overcoming this obstacle is to utilize the three-mirror folded resonator with an additional mirror to increase the loss difference between the lasing and competing channels. An alternative approach is the use of an intracavity selective absorber (ISA) in a simple linear cavity to absorb the competing emissions without introducing substantial losses at the lasing wavelength [7]. Therefore, the development of an ISA is practically beneficial to the power scaling of the weak transition in Nd-doped lasers.

In this Letter we demonstrate the development of an AlGaInAs material as a promising ISA for an efficient high-power Nd:YAG laser at 1.44 μm. With the ISA to suppress operation at 1.06 μm, the output coupling at 1.44 μm can be flexibly optimized; as a consequence, an output power of 2.5 W at 1.44 μm, with a slope efficiency of 23%, was achieved. We further verify that even if the cavity mirrors have a high-reflection coating at 1.06 μm, the developed ISA can still completely suppress the 1.06 μm oscillation and make a Nd:YAG laser cavity with an appropriate coupling to operate at 1.44 μm.

The present ISA was composed of AlGaInAs quantum wells (QWs) with the barrier structure grown on a Fe-doped InP transparent substrate by metalorganic chemical-vapor deposition. Note that the conventional S-doped InP substrate cannot be used because of its significant absorption in the 1.0–2.0 μm spectral region, whereas the Fe-doped InP substrate is transparent in this spectral region. The absorption region of the ISA consists of 10 groups of two 10 nm QWs with the absorption wavelength around 1.32 μm, spaced at 190 nm intervals by AlGaInAs barrier layers with the absorption wavelength around 1.06 μm, as shown in Fig. 1. An InP window layer was deposited on the gain structure to avoid surface recombination and oxidation. The backside of the substrate was mechanically polished after growth. Both sides of the gain chip were antireflection (AR)-coated to reduce backreflections. The total residual reflectivity of the AR-coated sample is less than 5%. Figure 2 shows the transmittance spectrum for the AR-coated ISA device. It can be seen that the strong absorption of the barrier layers leads to an extremely low transmittance near 1.06 μm. The total absorption efficiency of the barrier layers at 1.06 μm

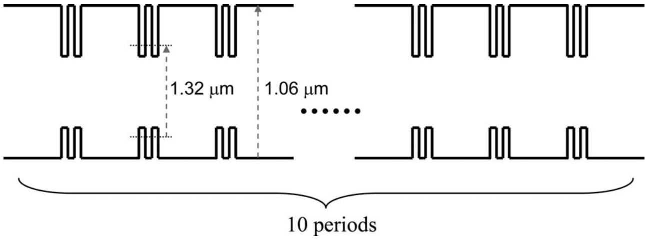

Fig. 1. Structure of the present ISA: the absorption region including 10 groups of two 10 nm QWs with the absorption wavelength around 1.32 μm, spaced at 190 nm intervals by AlGaInAs barrier layers with the absorption wavelength around 1.06 μm.

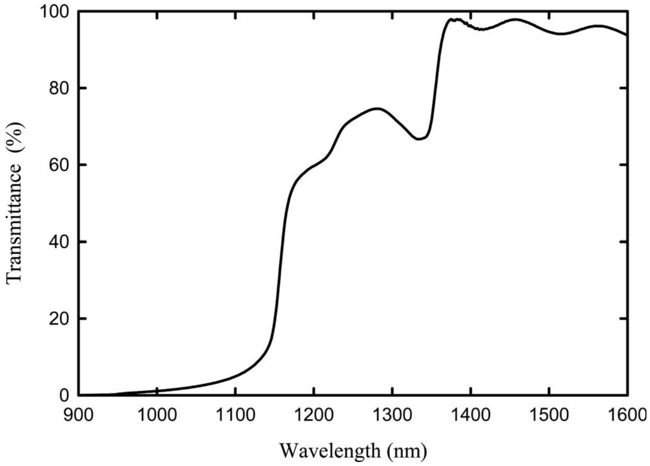

Fig. 2. Transmittance spectrum for the developed ISA device.

was found to be higher than 96%. On the other hand, the absorption efficiency of the AlGaInAs QWs near 1.32 μm was approximately 35%. Although the AlGaInAs material with a similar structure has been employed as a gain medium or a saturable absorber [8–12], it is designed as an ISA in solid-state lasers for the first time, to the best of our knowledge.

A schematic of the laser experiment is shown in Fig. 3. The active medium was 1.0 at. % Nd:YAG crystal with a length of 10 mm. The entrance surface of the laser crystal was coated for high reflection at 1.06 μm $(R > 99.5\%)$, 1.32 μm $(R > 99.5\%)$, and 1.44 μm $(R > 99.5\%)$ and for high transmission at 0.81 μm $(T > 85\%)$. Note that the high reflection at 1.06 and 1.32 μm on the entrance surface was for the purpose of exploring the suppression ability of the developed ISA. The other surface of the laser crystal was coated for AR in the spectral range of 1.06–1.44 μm $(R < 0.2\%)$. The laser crystal was wrapped with indium foil and mounted in a water-cooled copper block. The pump source was a 20 W 808 nm fiber-coupled laser diode with a core diameter of 600 μm and a numerical aperture of 0.16. A focusing lens with a 5 mm focal length and 85% coupling efficiency was used to reimage the pump beam into the laser crystal. The pump spot radius was approximately 200 μm. The cavity length was approximately 15 mm. The spectral information of the laser was monitored by an optical spectrum analyzer (Advantest Q8381A).

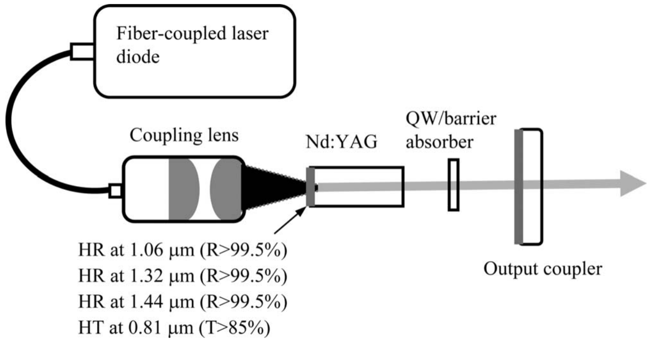

Fig. 3. Experimental schematic of the laser experiment.

Three different flat output couplers were used to test the function of the developed ISA. The first output coupler (OC1) was used to estimate the insertion loss of the ISA; its reflectivities at 1.06, 1.32, and 1.44 μm are 5%, 50%, and 99%, respectively. The loss difference of the OC1 for various transitions ensured that the oscillations at 1.06 and 1.32 μm were completely suppressed and the laser operated at 1.44 μm. Figure 4 shows the average output powers, with and without the ISA inserted into the cavity with the OC1, versus the incident pump power. The reduction in the slope efficiency due to the ISA can be seen to be rather small. With the Findlay–Clay analysis the insertion loss of the ISA is found to be approximately 0.2%. Note that the output efficiency with the OC1 is rather low because the output coupling is not optimal for the operation at 1.44 μm.

The second output coupler (OC2) was used to test the suppression ability of the ISA; its reflectivities at 1.06, 1.32, and 1.44 μm are 50%, 70%, and 95%, respectively. Experimental results reveal that the laser cavity with the OC2 and without the ISA is completely lasing at 1064 nm. With the insertion of the ISA, the laser cavity with the OC2 can be purely lasing at 1444 nm. Figure 5 shows the input–output characteristics for the output powers with and without the ISA inserted into the cavity with the OC2. It can be seen that the ISA can make the laser cavity to change the lasing wavelength from 1.06 to 1.44 μm. An output power of 2.5 W at 1.44 μm, with a slope efficiency of 23%, was achieved with the ISA inserted into the cavity with the OC2. At a pump power of 10 W the present output power is up to 1.7 W, which is superior to the previous data of 10 W obtained with a 2% output coupler [2,5]. The superiority comes from the advantage that an output coupler with a higher transmission can be used to optimize the output power because of the strong suppression at 1.06 μm transition by the ISA.

Finally, the third output coupler (OC3) was used to further investigate the maximum suppression ability of the ISA. The reflectivities of the OC3 at 1.32 and 1.44 μm are nearly the same as those of the OC2;

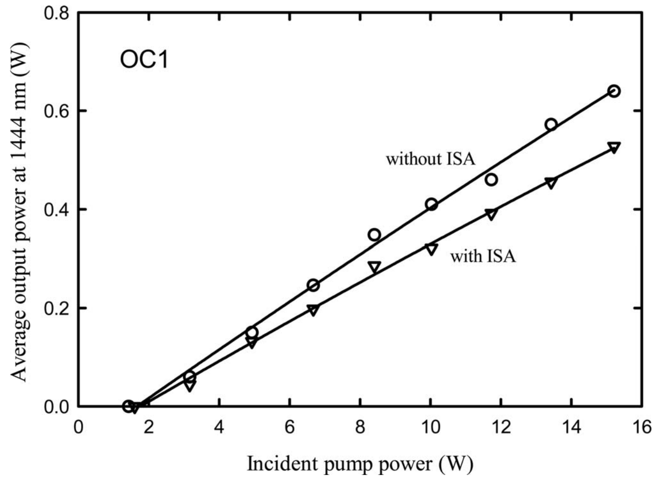

Fig. 4. Average output powers, with and without the ISA inserted into the cavity with the OC1, versus the incident pump power.

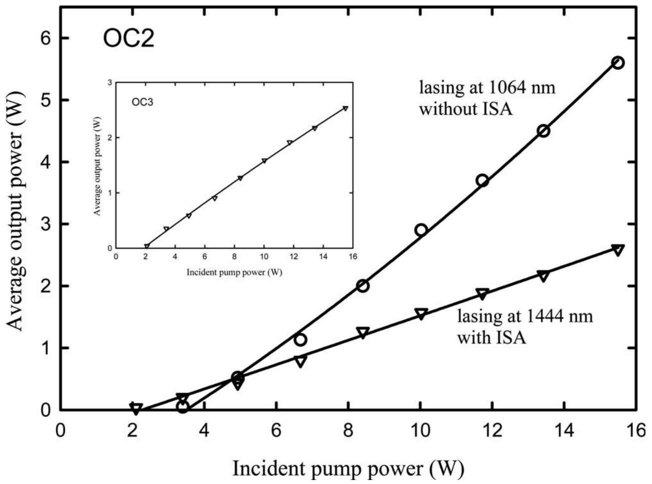

Fig. 5. Average output powers, with and without the ISA inserted into the cavity with the OC2, versus the incident pump power. Inset: average output power with ISA inserted into the cavity with the OC3.

however, the reflectivity of the OC3 at 1.06 μm is up to 99.5%. Experimental results reveal that the ISA can still suppress the 1.06 μm emission and lead to a Nd:YAG laser operating at 1.44 μm. More importantly, the output performance with the OC3 is almost the same as that obtained with the OC2, as seen in the inset of Fig. 5. In other words, the optimum output coupler at 1.44 μm can be straightforwardly designed by means of the ISA to suppress operation at 1.06 μm.

In summary, an AlGaInAs QW–barrier structure grown on a Fe-doped InP transparent substrate was developed to be an ISA for an efficient high-power Nd:YAG laser at 1.44 mm. Experimental results confirm that the developed ISA can still fully suppress the 1.06 μm oscillation even if the cavity mirrors have a high-reflection coating at 1.06 μm. With the ISA to suppress operation at 1.06 μm, the output coupler at 1.44 μm can be straightforwardly optimized. At a pump power of 16 W, an output power of 2.5 W at 1.44 μm, with a slope efficiency of 23%, was achieved.

The authors gratefully acknowledge various AlGaInAs/InP chips from TrueLight Corporation. The authors also thank the National Science Council for their financial support of this research under contract NSC-93-2112-M-009-034.

References

1. S. Singh, R. G. Smith, and L. G. Van Uitert, Phys. Rev. B **10**, 2566 (1974).
2. H. M. Kretschmann, F. Heine, V. G. Ostroumov, and G. Huber, Opt. Lett. **22**, 466 (1997).
3. N. Hodgson, W. L. Nighan, Jr. , D. J. Golding, and D. Eisel, Opt. Lett. **19**, 1328 (1994).
4. S. K. Wong, P. Mathieu, and P. Pace, Appl. Phys. Lett. **57**, 650 (1990).
5. A. Agnesi, S. Dell'Acqua, C. Pennacchio, G. Reali, and P. G. Gobbi, Appl. Opt. **37**, 3984 (1998).
6. J. Marling, IEEE J. Quantum Electron. **14**, 56 (1978).
7. I. V. Klimov, I. A. Shcherbakov, and V. B. Tsvetkov, Proc. SPIE **3829**, 165 (1999).
8. C. E. Zah, R. Bhat, B. N. Pathak, F. Favire, W. Lin, M. C. Wang, N. C. Andreadakis, D. M. Hwang, M. A. Koza, T. P. Lee, Z. Wang, D. Darby, D. Flanders, and J. J. Hsieh, IEEE J. Quantum Electron. **30**, 511 (1994).
9. N. Nishiyama, C. Caneau, B. Hall, G. Guryanov, M. H. Hu, X. S. Liu, M.-J. Li, R. Bhat, and C. E. Zah, IEEE J. Sel. Top. Quantum Electron. **11**, 990 (2005).
10. O. Hanaizumi, K. T. Jeong, S. Y. Kashiwada, I. Syuaib, K. Kawase, and S. Kawakami, Opt. Lett. **21**, 269 (1996).
11. K. W. Su, S. C. Huang, A. Li, S. C. Liu, Y. F. Chen, and K. F. Huang, Opt. Lett. **31**, 2009 (2006).
12. S. C. Huang, S. C. Liu, A. Li, K. W. Su, Y. F. Chen, and K. F. Huang, Opt. Lett. **32**, 1480 (2007).